

# LOW-FREQUENCY VIBRATIONS OF DNA WITH COUNTERIONS IN CROSS-STRANDED POSITION

S.M. PEREPELYTSYA, S.N. VOLKOV

PACS 87.14.Gg, 87.15.-v,  
87.15.He  
©2010

Bogolyubov Institute for Theoretical Physics, Nat. Acad. of Sci. of Ukraine  
(14-b Metrolohichna Str., Kyiv 03680, Ukraine)

Low-frequency vibrations of DNA with counterions between phosphate groups of different strands of the double helix are studied in the framework of a developed phenomenological model. The frequencies, amplitudes, and Raman intensities of DNA modes in the frequency interval from 10 to 200  $\text{cm}^{-1}$  are calculated for the case of  $\text{Mg}^{2+}$  counterions at different positions with respect to the double helix strands (near or between phosphate groups). The calculations show that the counterions between phosphate groups influence the modes of H-bond stretching in the base pairs and the modes of backbone vibrations mostly. Using the calculated intensities and the frequencies of vibrations, the low-frequency Raman spectra of Mg-DNA are built. The obtained spectra allow us to distinguish the positions of counterions with respect to the phosphate groups of the DNA double helix.

tracted from the low-frequency ( $<200 \text{ cm}^{-1}$ ) spectra of DNA in solutions. This spectral range is characteristic of transverse vibrations of the double helix structural elements [22–26]. We have found that the vibrations of counterions with respect to the phosphate groups (ion-phosphate vibrations) also fall in the low-frequency range. The ion-phosphate vibrations are interconnected with the modes of DNA low-frequency vibrations and can influence the internal dynamics of a double helix. The frequency and the intensity of ion-phosphate modes depend on the counterion type and the structure of a double helix that is confirmed by experimental data [27–30].

## 1. Introduction

The indispensable condition of the DNA double helix structure in a solution is the presence of metal counterions that neutralize the negatively charged phosphate groups of the macromolecule backbone. The counterions together with water molecules form the ion-hydrate shell around the double helix [1]. The disposition of counterions, their type and concentration in the shell determine the mechanisms of such important processes as the nucleic-protein recognition, interaction with biologically active compounds, helix-coil transition, *etc.* [2–7].

In a water solution, only the average picture of the ion-hydrate shell can be determined experimentally [8–11]. On the other hand, the computational methods give the information about probable localization sites of counterions in a DNA macromolecule and respective residence times only [12–16], which is insufficient for the interpretation of experimental data and the understanding of the mechanisms of DNA functioning. So, the development of methods of determination of the positions of counterions in the DNA ion-hydrate shell is urgently needed.

In our works [17–21], it was demonstrated that the information about a disposition of counterions and their influence on the DNA vibrational dynamics can be ex-

The case where each counterion is tethered only to one phosphate group (single-strand neutralization) has been considered in our previous works [17–21]. At the same time, the experimental and computational data [5, 31–35] show that the counterions can be also localized between phosphate groups of different strands of the double helix (cross-strand neutralization). For example,  $\text{Mg}^{2+}$  ions are the most likely for the disposition between cross-strand phosphate groups [5, 31, 32].

In the present work, the vibrations of DNA with  $\text{Mg}^{2+}$  counterions in different positions with respect to the double helix phosphate groups are studied. The model describing the low-frequency vibrations of DNA with counterions is extended, and the frequencies, amplitudes, and the Raman intensities of DNA models lower than 200  $\text{cm}^{-1}$  are estimated for the case of  $\text{Mg}^{2+}$  counterions. The obtained results show that the counterion localization essentially influences the low-frequency modes of the DNA double helix.

## 2. Model of Low-frequency Vibrations of DNA with Counterions in Cross-stranded Position

The cross-stranded localization of counterions is favorable in the case of short distances between phosphates of different DNA strands (about  $7\div 10 \text{ \AA}$ ) [5, 31–35]. Such distances can be realized in different conformations of the double helix, for example, in the case of *A*-, *D*-

and  $Z$ -forms of DNA [2]. In these conformations, the counterions are localized in grooves of the double helix and coordinate several phosphate groups. In the present work, we consider the case where the counterion is localized in the minor groove of the double helix between phosphate groups of the same monomer link.

At a sufficient concentration of ions in a solution, the localization of counterions along a DNA macromolecule can be rather regular, since the backbone of the double helix has a uniform structure. Therefore, such a structure has been considered in our previous works [17–19] as an ionic lattice (ion-phosphate lattice). Following this conception, we consider the double helix with counterions in the cross-stranded position as a partial case of the ion-phosphate lattice.

The internal dynamics of the DNA ion-phosphate lattice is described with the use of the four-mass model [22–26]. In the framework of this model, the phosphate groups of DNA are considered as masses located on the strands of the double helix ( $m_0$ :  $\text{PO}_2 + 2\text{O} + \text{C}'_5$ ). The bases with deoxyribose rings (nucleosides) are considered as the physical pendulums with mass  $m$  and reduced length  $l$  that are coupled by the elastic forces (H-bonds) at the center of the double helix. The counterions are represented as the masses  $m_a$  that are localized between cross-strand phosphate groups of the monomer link (Fig. 1, a).

The displacements of nucleosides and phosphate groups in a DNA monomer link are described by means of  $X_{i1}$ ,  $X_{i2}$ ,  $Y_{i1}$ , and  $Y_{i2}$  coordinates (Fig. 1, b). The rotational vibrations of pendulum-nucleosides with respect to the phosphate groups are described by deviations  $\theta_{i1}$  and  $\theta_{i2}$  from the angle  $\theta_{eq}$  describing their equilibrium position in the plane of the complementary DNA pair. The deoxyribose and the base vibrate respectively each other inside the nucleoside (intranucleoside vibrations), which is described by changes of the pendulum lengths  $\rho_{i1}$  and  $\rho_{i2}$ . The vibrations of counterions are described by the coordinate  $\xi_i$ . The motions of structural elements of a monomer link are considered in a plane orthogonal to the helical axis.

The energy of low-frequency vibrations of DNA with counterions can be written in the form

$$E = \sum_i (E_h^i + E_c^i + E_{i,i+1}), \quad (1)$$

where  $E_h^i$  is the monomer link energy;  $E_c^i$  is the energy of counterions tethered to the phosphate groups;  $E_{i,i+1}$  is the interaction energy of the structure elements along the double helix;  $i = 0, \pm 1 \dots \pm N$  (Fig. 1, a).

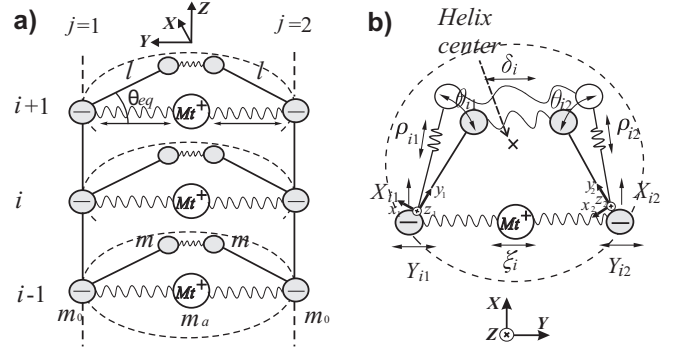


Fig. 1. The model of low-frequency vibrations of DNA with counterions in the cross-stranded position. a) The double chain of nucleotides with counterions.  $l$  is the reduced length of a pendulum-nucleoside;  $\theta_{eq}$  is the equilibrium angle;  $i$  and  $j$  enumerate monomer links and chains of the double helix, respectively;  $m$ ,  $m_0$ , and  $m_a$  are the masses of nucleosides, phosphate groups, and counterions, respectively. b) Monomer link of the model shown in a plane orthogonal to the helical axis.  $X_{ij}$ ,  $Y_{ij}$ ,  $\theta_{ij}$ ,  $\rho_{ij}$ , and  $\xi_i$  are the coordinates of vibrations (see text);  $\delta_i$  is the H-bond stretching in base pairs

The energy of vibrations of structural elements in a monomer link  $i$  of the DNA double helix has been determined in the framework of four-mass model [22–26] as follows:

$$E_h^i = \sum_j \frac{M}{2} (\dot{X}_{ij}^2 + \dot{Y}_{ij}^2) + \sum_j \frac{m}{2} [\dot{\rho}_{ij}^2 + l^2 \dot{\theta}_{ij}^2 + 2l\dot{\theta}_{ij}(\dot{Y}_{ij}a + \dot{X}_{ij}b) + 2\dot{\rho}_{ij}(\dot{Y}_{ij}b - \dot{X}_{ij}a)] + \frac{\alpha}{2} \delta_i^2 + \frac{1}{2} \sum_{j=1}^2 (\sigma \rho_{ij}^2 + \beta \theta_{ij}^2), \quad (2)$$

where index  $j$  enumerates chains of the double helix;  $M = m_0 + m$  is the nucleotide mass;  $a = \sin \theta_{eq}$ ;  $b = \cos \theta_{eq}$ ;  $\alpha$ ,  $\sigma$ , and  $\beta$  are the force constants of H-bond stretching in base pairs, intranucleoside mobility, and rotation of nucleosides with respect to the backbone chain in the base-pair plane, respectively; the variable  $\delta_i$  describes the stretching of H-bonds in the base pairs and is determined here in the same way as in [23–26]:

$$\delta_i \approx la(\theta_{i1} + \theta_{i2}) + Y_{i2} + Y_{i1} + b(\rho_{i1} + \rho_{i2}). \quad (3)$$

The energy of counterion vibrations in the case of the cross-strand neutralization can be written as

$$E_c^i = \sum_j \left[ \frac{m_a}{2} \dot{\xi}_i^2 + \frac{\gamma}{2} (Y_{ij} + (-1)^j \xi_i)^2 \right], \quad (4)$$

where  $\gamma$  is the force constant of counterion vibrations.

The term  $E_{i,i+1}$  in formula (1) describes the interactions between the neighboring monomers in the chain. According to our approach [17–19], we will consider the limited long-wave vibrational modes of the ion-phosphate lattice that are sufficient for the interpretation of the experimental vibrational spectra. As known, only long-range lattice vibrations interact with the electromagnetic fields and manifest itself in vibrational spectra [36]. In long-wave limit, when the wave vector tends to zero ( $\bar{k} \rightarrow 0$ ), the frequencies of optical-type modes weakly depend on  $\bar{k}$ . In the theory of lattice vibrations, such an approximation is the same as the neglect of the interaction along the chain. So, in the following consideration, we will neglect the interaction term:  $E_{i,i+1} \approx 0$ .

On the basis of formulas (1)–(4), we can write the equations of motion for the system. In the variables  $X_i = X_{i1} + X_{i2}$ ,  $x_i = X_{i1} - X_{i2}$ ,  $Y_i = Y_{i1} + Y_{i2}$ ,  $y_i = Y_{i1} - Y_{i2}$ ,  $\theta_i = \theta_{i1} + \theta_{i2}$ ,  $\eta_i = \theta_{i1} - \theta_{i2}$ ,  $\rho_i = \rho_{i1} + \rho_{i2}$ ,  $u_i = \rho_{i1} - \rho_{i2}$ , and  $\xi_i = \xi_i$ , the system of equations of motion splits into two subsystems of coupled equations. The first subsystem consists of 4 equations with respect to  $X_i$ ,  $Y_i$ ,  $\theta_i$ , and  $\rho_i$  coordinates describing symmetric long-wave vibrations in the DNA monomer link. The second subsystem consists of 5 equations with respect to  $x_i$ ,  $y_i$ ,  $\eta_i$ ,  $u_i$ , and  $\xi_i$  coordinates characterizing antisymmetric long-wave vibrations in the DNA monomer link.

To find the normal vibrations of the system, we search for solutions of the equations of motions in the form  $q_i = \tilde{q}_i \cos(\omega t)$ , where  $q_i = \{X_i, x_i, Y_i, y_i, \theta_i, \eta_i, \rho_i, u_i, \xi_i\}$  and  $\tilde{q}_i = \{\tilde{X}_i, \tilde{x}_i, \tilde{Y}_i, \tilde{y}_i, \tilde{\theta}_i, \tilde{\eta}_i, \tilde{\rho}_i, \tilde{u}_i, \tilde{\xi}_i\}$  are the coordinates and the amplitudes of displacements, respectively. The resulted equations for the frequencies of normal vibrations of the system in a long-wave limit have the form

$$\left\{ \begin{array}{l} \tilde{Y}_i (\alpha_0 + \gamma_0 \frac{m_a}{M} - \omega^2) + \\ + (\tilde{\rho}_i b + \tilde{\theta}_i l a) (\alpha_0 \frac{M}{m} - \omega^2) \frac{m}{M} = 0; \\ \tilde{X}_i - (\tilde{\rho}_i a - \tilde{\theta}_i l b) \frac{m}{M} = 0; \\ \tilde{Y}_i a (\alpha_0 \frac{M}{m} - \omega^2) - (\tilde{X}_i \omega^2 - \tilde{\rho}_i \alpha_0 \frac{M}{m} a) b + \\ \tilde{\theta}_i l (\alpha_0 \frac{M}{m} a^2 + \beta_0 - \omega^2) = 0; \\ \tilde{Y}_i b (\alpha_0 \frac{M}{m} - \omega^2) + (\tilde{X}_i \omega^2 + \tilde{\theta}_i \alpha_0 \frac{M}{m} l b) a + \\ + \tilde{\rho}_i (\alpha_0 \frac{M}{m} b^2 + \sigma_0 - \omega^2) = 0; \end{array} \right. \quad (5)$$

$$\left\{ \begin{array}{l} \tilde{y}_i (\gamma_0 \frac{m_a}{M} - \omega^2) - \\ - (\tilde{u}_i b + \tilde{\eta}_i l a) \omega^2 \frac{m}{M} - 2\tilde{\xi}_i \gamma_0 \frac{m_a}{M} = 0; \\ \tilde{x}_i - (\tilde{u}_i a - \tilde{\eta}_i l b) \frac{m}{M} = 0; \\ \tilde{y}_i a \omega^2 + \tilde{x}_i \omega^2 b - \tilde{\eta}_i l (\beta_0 - \omega^2) = 0; \\ \tilde{y}_i b \omega^2 - \tilde{x}_i \omega^2 a - \tilde{u}_i (\sigma_0 - \omega^2) = 0; \\ \tilde{y}_i \gamma_0 - \tilde{\xi}_i (2\gamma_0 - \omega^2) = 0; \end{array} \right. \quad (6)$$

where  $\alpha_0 = 2\alpha/M$ ;  $\beta_0 = \beta/ml^2$ ;  $\sigma_0 = \sigma/m$ ;  $\gamma_0 = \gamma/m_a$ .

Using the existence condition for a solution of Eqs. (5) and (6), we determined the frequencies of long-wave vibrations. The system of equations (5) gives 4 modes of vibrations. Three of them are of the optical type and one of the acoustic type. The modes of the optical type describe symmetric motions of the double helix backbone ( $\omega_B^+$ ) and the stretching of H-bonds in base pairs ( $\omega_H^+$  and  $\omega_{HS}^+$ ). The system of equations (6) gives 5 modes of vibrations. Three of them are of the optical type and two of the acoustic type. The modes of the optical type describe antisymmetric vibrations of the double helix backbone ( $\omega_B^-$ ), intranucleoside vibrations ( $\omega_S^-$ ), and ion-phosphate vibrations ( $\omega_{Ion}^-$ ). As we can see in the case of cross-strand neutralization, there is only one mode of antisymmetric ion-phosphate vibrations  $\omega_{Ion}^-$ , while, in the case of single-strand neutralization, there is also the symmetric ion-phosphate mode  $\omega_{Ion}^+$  [17–19]. The frequencies of the acoustic modes are equal to zero in our case, since we consider the limited long-range vibrations.

To analyze the character of DNA low-frequency vibrations, we found the analytical forms for the modes  $\omega_H^+$ ,  $\omega_B^+$ ,  $\omega_{Ion}^-$ , and  $\omega_B^-$  using the rigid nucleoside approximation of the four-mass model [22]. In the framework of this approximation, vibrations of the phosphate groups along the Y-axis (the coordinates  $Y$  and  $y$ ) and the vibrations of pendulum-nucleosides (the coordinates  $\theta$  and  $\eta$ ) are considered only. The resulted formulas show that the frequencies of symmetric vibrations depend on all force constants of the model. In contrast, the modes of antisymmetric vibrations depend only on some definite force constant determining the motions of structural elements. So, the modes of symmetric vibrations of a DNA double helix should be sensitive to the counterion localization, whereas the modes of antisymmetric vibrations should be the same as those in the case of the four-mass model without counterions [22–26].

### 3. Frequencies and Amplitudes of Vibrations of DNA with Counterions

To calculate the frequencies and the amplitudes of vibrations, we considered the cases of DNA with  $Mg^{2+}$  counterions in cross-stranded and single-stranded positions. A  $Mg^{2+}$  ion is known to be highly hydrated [37]. Therefore, it is considered together with the hydration shell consisting of 6 water molecules. The size of the  $[Mg(H_2O)_6]^{2+}$  complex and its charge suit the best for the localization between phosphate groups of a DNA monomer link.

The force constants  $\alpha$ ,  $\sigma$ , and  $\beta$  and the reduced length  $l$  are taken the same as those in the four-mass model for B-DNA [22–26]. The equilibrium angle  $\theta_{eq}$  in the case of cross-strand neutralization is determined from the geometry of a monomer link with the distance between phosphates 8.5 Å that corresponds to the experimental data [32]. The estimated value is  $\theta_{eq} = 55^\circ$  that is essentially higher than that in the case of the model of DNA with single-stranded counterions [17–19]. The constants  $\gamma$  for DNA with hydrated  $Mg^{2+}$  counterions in different positions with respect to the phosphate groups are calculated using the approach developed in [19]. In the framework of this approach, the ion-phosphate interaction is considered analogously to the interaction of ions in an ionic lattice. The ion-hydrate shell of DNA with counterions is taken into consideration by the dielectric constant and the Madelung constant of the ion-phosphate lattice. The dielectric constant is considered the same as that for Na-DNA [19]. The distance between a counterion and a phosphate group is taken equal to 4.25 Å according to the experimental data [32]. According to our estimations, the Madelung constant is close to 1. The obtained value of the constant  $\gamma$  for DNA with  $[Mg(H_2O)_6]^{2+}$  counterions in cross-stranded and single-stranded positions is 45 kcal/molÅ<sup>2</sup>.

To determine a character of low-frequency vibrations for DNA with hydrated  $Mg^{2+}$  counterions in the single-stranded position, we calculated the amplitudes of vibrations in the same way as in [18, 19]. For DNA with hydrated  $Mg^{2+}$  counterions in the cross-stranded position, the following expressions are obtained analogously

**Table 1. The frequencies of Mg-DNA conformational vibrations for the case of counterions in the cross-stranded and single-stranded positions (cm<sup>-1</sup>)**

Mode	$\omega_{Ion}^+$	$\omega_H^+$	$\omega_B^+$	$\omega_{HS}^+$	$\omega_{Ion}^-$	$\omega_S^-$	$\omega_B^-$
Cross-strand	—	108	54	84	118	78	15
Single-strand	126	102	13	43	123	61	12

to [18, 19]:

$$\tilde{\theta} = 2\sqrt{\frac{k_B T}{E_0^+}}; \quad \tilde{\eta} = 2\sqrt{\frac{k_B T}{E_0^-}}. \quad (7)$$

Here,  $k_B$  is the Boltzmann constant,  $T$  is the temperature (300 K), and

$$E_0^+ = 2\alpha \left( \frac{\tilde{Y}}{\tilde{\theta}} + la + b\frac{\tilde{\rho}}{\tilde{\theta}} \right)^2 + \beta + \sigma \left( \frac{\tilde{\rho}}{\tilde{\theta}} \right)^2 + \gamma \left( \frac{\tilde{Y}}{\tilde{\theta}} \right)^2;$$

$$E_0^- = \beta + \sigma \left( \frac{\tilde{u}}{\tilde{\eta}} \right)^2 + \gamma \left( \frac{\tilde{y}}{\tilde{\eta}} - 2\frac{\tilde{\xi}}{\tilde{\eta}} \right)^2. \quad (8)$$

The ratio between amplitudes in (7) and (8) can be determined from Eqs. (5) and (6).

The frequencies and the amplitudes of vibrations for DNA with counterions in the cross-stranded position are calculated, by using formulae (5)–(8). To compare the character of DNA conformational vibrations under different counterion localizations, the frequencies and the amplitudes of vibrations of Mg-DNA with counterions in the single-stranded position are determined, by also using the scheme developed in our previous work [18, 19].

The calculated frequencies of vibrations (Table 1) show that the counterions in the cross-stranded position influence the frequencies of symmetric vibrations  $\omega_H^+$ ,  $\omega_{HS}^+$ , and  $\omega_B^+$ . The frequency  $\omega_H^+$  becomes slightly higher, the frequency  $\omega_{HS}^+$  increases about twice, and the frequency  $\omega_B^+$  increases by several times, as compared with the case of DNA with  $Mg^{2+}$  counterions in the single-stranded position. The frequencies of anti-symmetric backbone vibrations  $\omega_B^-$  and intranucleoside vibrations  $\omega_S^-$  in the case of cross-strand neutralization are practically the same as those in the case of DNA without counterions [23–26]. The calculated frequencies of vibrations of DNA with  $Mg^{2+}$  counterions in the single-stranded position are close to the frequencies of Cs-DNA obtained in our previous work [19], which is due to high masses of Cs<sup>+</sup> and hydrated  $[Mg(H_2O)_6]^{2+}$  ions. The frequencies of ion-phosphate vibrations are close to 120 cm<sup>-1</sup> for both cases of counterion localization.

The calculated amplitudes of vibrations (Table 2) show that the character of low-frequency vibrations of a double helix depends essentially on the counterion localization with respect to the phosphate groups. The mode of symmetric backbone vibrations  $\omega_B^+$  in the case of cross-strand neutralization is characterized by smaller

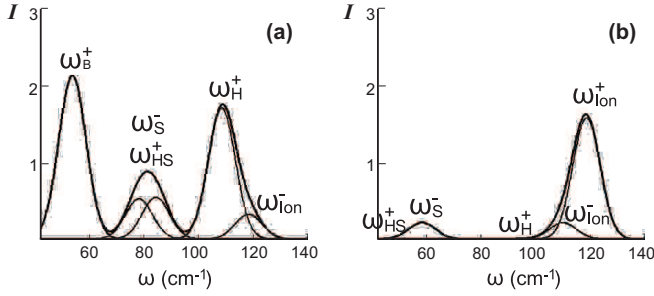


Fig. 2. The calculated low-frequency Raman spectra of DNA with  $Mg^{2+}$  counterions in the cross-stranded (a) and single stranded (b) positions. The half-width of the spectral lines is  $5 \text{ cm}^{-1}$ . Heavy line shows the resulted spectra.  $I$  is the relative intensity

amplitudes of vibrations as compared with the case of single-strand neutralization. The exception is the amplitude of intranucleoside vibrations that is high. Therefore, this mode may be considered as the mode of intranucleoside vibrations as well. The mode of antisymmetric backbone vibrations  $\omega_B^-$  in the case of cross-stranded neutralization has high amplitudes of phosphate ( $\tilde{x}$  and  $\tilde{y}$ ) and pendulum-nucleoside ( $\tilde{\eta}$ ) vibrations in both cases of counterion localization. The mode  $\omega_S^-$  is characterized by a large amplitude of intranucleoside vibrations ( $\tilde{u}$ ) that is higher in the case of cross-strand neutralization. The modes of H-bond stretching  $\omega_H^+$  and  $\omega_{HS}^+$  are characterized by large amplitudes of intranucleoside vibrations ( $\tilde{\rho}$ ) and the H-bond stretching ( $\tilde{\delta}$ ) for both considered cases of counterion localization. The mode of ion-phosphate vibrations  $\omega_{Ion}^-$  in the case of counterions in the cross-stranded position is characterized by the displacements of counterions and by the intranucleoside mobility the same as that in the case of single-stranded counterions. In the case of single-stranded counterions, the mode  $\omega_{Ion}^+$  is also characterized by the H-bond stretching in the base pairs ( $\tilde{\delta}$ ), which is due to the high mass of hydrated  $Mg^{2+}$  counterions (132 a.u.m.).

#### 4. Intensities of the Raman Modes of DNA with Counterions

To determine the low-frequency Raman spectra, the intensities of DNA modes are calculated in the framework of a phenomenological approach developed in our works [20, 21]. The approach is based on the valence-optic theory [38] and our model for DNA conformational vibrations with counterions [17–19]. According to this approach, the intensity of some DNA mode that is observed in the Stokes part of a Raman spectrum at the

right-angle geometry is determined as follows [20, 21]:

$$J_n \approx \frac{3\kappa J_0 (\nu_0 - \nu_n)^4}{1 - \exp(-\frac{h\nu_n}{k_B T})} \left[ \left( \sum_{j=1}^2 A_j^n \right)^2 + \left( \sum_{j=1}^2 B_j^n \right)^2 \right], \quad (9)$$

$$A_j^n = [(b_{jyy} - b_{jxx})\vartheta_s + 2(-1)^j b_{jxy}\vartheta_c](\tilde{\theta}_j^n + \tilde{\rho}_j^n/l),$$

$$B_j^n = [(b_{jyy} - b_{jxx})(-1)^j\vartheta_c - 2b_{jxy}\vartheta_s](\tilde{\theta}_j^n + \tilde{\rho}_j^n/l),$$

where  $\kappa = 13 \times 28\pi^5/(9c^4)$ ;  $J_0$  and  $\nu_0$  are, respectively, the intensity and the frequency of incident light;  $\nu_n = \omega_n/2\pi$  is the frequency of molecular normal vibrations; index  $n$  means the mode of normal vibrations;  $c$  is the velocity of light;  $h$  is the Planck constant;  $b_{jxx}$ ,  $b_{jxy}$ , and  $b_{jyy}$  are the components of the nucleoside polarizability tensor;  $\vartheta_s = \sin 2\theta_{eq}$ ; and  $\vartheta_c = \cos 2\theta_{eq}$ .

In calculating the mode intensities by formulae (9), the necessary polarizabilities of nucleosides are estimated with the help of the bond polarizability scheme [39]. The frequencies and the amplitudes of vibrations for the case of DNA with  $Mg^{2+}$  counterions in the cross-stranded and single-stranded positions are taken from Tables 1 and 2. As a result, the calculated spectra for Mg-DNA at different counterion localizations with respect to the phosphate groups are built (Fig. 2).

The calculations show that, at frequencies higher than  $50 \text{ cm}^{-1}$ , three bands are observed in the spectrum of

**Table 2. The amplitudes of Mg-DNA conformational vibrations for the case of counterions in the cross-stranded and single-stranded positions**

Cross-strand								
Mode	–	$\omega_H^+$	$\omega_B^+$	$\omega_{HS}^+$	Mode	$\omega_{Ion}^-$	$\omega_S^-$	$\omega_B^-$
$\tilde{Y}$ (pm)	–	5	–20	–6	$\tilde{y}$ (pm)	2	–14	–44
$\tilde{X}$ (pm)	–	–6	–17	14	$\tilde{x}$ (pm)	–9	3	–52
$\tilde{\theta}$ (°)	–	1	4	0	$\tilde{\eta}$ (°)	1	1	14
$\tilde{\rho}$ (pm)	–	14	–14	–12	$\tilde{u}$ (pm)	9	–22	1
$\tilde{\delta}$ (pm)	–	9	3	7	$\tilde{\xi}$ (pm)	6	6	–27

Single-strand*								
Mode	$\omega_{Ion}^+$	$\omega_H^+$	$\omega_B^+$	$\omega_{HS}^+$	Mode	$\omega_{ion}^-$	$\omega_S^-$	$\omega_B^-$
$\tilde{Y}$ (pm)	–10	5	–59	–14	$\tilde{y}$ (pm)	–11	5	–25
$\tilde{X}$ (pm)	1	0	–47	–11	$\tilde{x}$ (pm)	1	–5	–48
$\tilde{\theta}$ (°)	1	0	14	2	$\tilde{\eta}$ (°)	1	0	14
$\tilde{\rho}$ (pm)	13	5	2	–19	$\tilde{u}$ (pm)	12	–20	0
$\tilde{\xi}_+$ (pm)	15	–11	–2	7	$\tilde{\xi}_-$ (pm)	17	10	–1
$\tilde{\delta}$ (pm)	5	10	–1	6				

\*  $\tilde{\xi}_+ = \tilde{\xi}_1 + \tilde{\xi}_2$  and  $\tilde{\xi}_- = \tilde{\xi}_1 - \tilde{\xi}_2$ , where  $\tilde{\xi}_1$  and  $\tilde{\xi}_2$  describe the vibrations of counterions that are tethered to the first ( $j = 1$ ) and the second ( $j = 2$ ) DNA strands, respectively.

DNA with  $\text{Mg}^{2+}$  counterions in the cross-strand position. The band near  $55 \text{ cm}^{-1}$  arises due to the mode of backbone vibrations ( $\omega_B^+$ ). The modes of intranucleoside vibrations ( $\omega_S^-$ ) and H-bond stretching in base pairs ( $\omega_{HS}^+$ ) form the band near  $80 \text{ cm}^{-1}$ , and the modes of H-bond stretching in base pairs ( $\omega_H^+$ ) and ion-phosphate vibrations ( $\omega_{\text{Ion}}^-$ ) form the band near  $110 \text{ cm}^{-1}$  (Fig. 2, *a*).

In the spectrum of Mg-DNA with counterions in the single-stranded position, the mode of ion-phosphate vibrations  $\omega_{\text{Ion}}^+$  near  $120 \text{ cm}^{-1}$  is the most intensive. This is due to the high mass of hydrated  $\text{Mg}^{2+}$  counterions, which disturbs the vibrations of internal structural elements of the double helix. Other modes have low intensities (Fig. 2, *b*). The structure of the Mg-DNA spectrum in this case resembles that of the spectrum of Cs-DNA [20, 21]. The obtained results show that the spectra of Mg-DNA essentially depend on the counterion localization with respect to phosphate groups of the double helix.

## 5. Conclusions

An approach for the description of the low-frequency vibrations of DNA with counterions in different positions with respect to the double helix strands is developed. Using this approach, the frequencies, amplitudes, and Raman intensities are determined for DNA with hydrated  $\text{Mg}^{2+}$  counterions in the single-stranded and cross-stranded positions. Note that the calculated frequencies of internal vibrations of the double helix are sensitive to the counterion localization. In the case of cross-strand neutralization of phosphate groups, the frequencies of the H-bond stretching in base pairs and the frequency of backbone vibrations are much higher than those in the case of single-strand neutralization. The calculated amplitudes of vibrations show that the characters of DNA conformational vibrations are essentially different in the case of cross-stranded and single stranded positions of counterions. The calculated low-frequency Raman spectra of Mg-DNA are strongly different in the case of single-strand and cross-strand neutralizations. This difference arises due to the DNA conformational changes and to the influence of counterions. The obtained low-frequency Raman spectra of Mg-DNA allow us to distinguish the positions of counterions with respect to the phosphate groups of the double helix.

1. G.S. Manning, *Q. Rev. Biophys.* **11**, 179 (1978).
2. W. Saenger, *Principles of Nucleic Acid Structure* (Springer, New York, 1984).

3. C.G. Baumann, S.B. Smith, V.A. Bloomfield, and C. Bustamante, *Proc. Natl. Acad. Sci. USA* **94**, 6185 (1997).
4. L.D. Williams and L.J. Maher III, *Annu. Rev. Biophys. Biomol. Struct.* **29**, 497 (2000).
5. N.V. Hud and M. Polak, *Current Opinion Struct. Biol.* **11**, 293 (2001).
6. Y. Levin, *Rep. Prog. Phys.* **65**, 1577 (2002).
7. A.A. Kornyshev, D.J. Lee, S. Leikin, and A. Wynveen, *Rev. Mod. Phys.* **79**, 943 (2007).
8. R. Das, T.T. Mills, L.W. Kwok *et al.*, *Phys. Rev. Lett.* **90**, 188103 (2003).
9. K. Andersen, R. Das, H.Y. Park *et al.*, *Phys. Rev. Lett.* **93**, 248103 (2004).
10. K. Andresen, X. Qui, S.A. Pabit *et al.*, *Biophys. J.* **95**, 287 (2008).
11. X. Qiu, L.W. Kwok, H.Y. Park *et al.*, *Phys. Rev. Lett.* **101**, 228101 (2008).
12. N. Korolev, A.P. Lyubartsev, A. Laaksonen, and L. Nordenskiöld, *Nucl. Acids Res.* **31**, 5971 (2003).
13. P. Varnai and K. Zakrzewska, *Nucleic Acids Res.* **32**, 4269 (2004).
14. S.Y. Ponomarev, K.M. Thayer, and D.L. Beveridge, *Proc. Natl. Acad. Sci. USA* **101**, 14771 (2004).
15. Y. Cheng, N. Korolev, and L. Nordenskiöld, *Nucl. Acids Res.* **34**, 686 (2006).
16. S. Sen, D. Andreatta, S.Y. Ponomarev *et al.*, *J. Am. Chem. Soc.* **131**, 1724 (2009).
17. S.M. Perepelytsya and S.N. Volkov, *Ukr. J. Phys.* **49**, 1072 (2004); arXiv: q-bio.BM/0412022.
18. S.M. Perepelytsya and S.N. Volkov, *Biophys. Bull.* **15**(1), 5 (2005) [Kharkov].
19. S.M. Perepelytsya and S.N. Volkov, *Eur. Phys. J. E* **24**, 261 (2007).
20. S.M. Perepelytsya and S.N. Volkov, *Biophys. Bull.* **23**(2), 5 (2009) [Kharkov]; arXiv: q-bio.BM/0805.0696v1.
21. S.M. Perepelytsya and S.N. Volkov, *Eur. Phys. J. E* **31**, 201 (2010).
22. S.N. Volkov and A.M. Kosevich, *Molek. Biol.* **21**, 797 (1987).
23. S.N. Volkov, A.M. Kosevich, and G.E. Weinreb, *Biopolim. i Kletka* **5**, 32 (1989).
24. S.N. Volkov and A.M. Kosevich, *J. Biomol. Struct. Dyn.* **8**, 1069 (1991).
25. S.N. Volkov, *Biopol. i Kletka* **7**, 40 (1991).

26. A.M. Kosevich and S.N. Volkov, in *Nonlinear Excitations in Biomolecules*, edited by M. Peyrard (Springer, New York, 1995), Chapter 9.
27. J.W. Powell, G.S. Edwards, L. Genzel *et al.*, Phys. Rev. A **35**, 3929 (1987).
28. T. Weidlich, S.M. Lindsay, Qi Rui *et al.*, J. Biomol. Struct. Dyn. **8**, 139 (1990).
29. T. Weidlich, J.W. Powell, L. Genzel, and A. Rupprecht, Biopolymers **30**, 477 (1990).
30. L.A. Bulavin, S.N. Volkov, S.Yu. Kutovyi, and S.M. Perepeelytsya, Dopov. Nats. Akad. Nauk Ukr.h **10**, 69 (2007); arXiv: q-bio.BM/0805.0696v1.
31. V. Tereshko, G. Minasov, and M. Egli, J. Am. Chem. Soc. **121**, 470 (1999).
32. C.C. Sines, L. McFail-Isom, S.B. Howerton, D. VanDerveer, and L.D. Williams, J. Am. Chem. Soc. **122**, 11048 (2000).
33. D. Hamelberg, L. McFail-Isom, L.D. Williams, and W.D. Wilson, J. Am. Chem. Soc. **122**, 10513 (2000).
34. S.B. Howerton, C.C. Sines, D. VanDerveer, and L.D. Williams, Biochemistry **40**, 10023 (2001).
35. D. Hamelberg, L.D. Williams, and W.D. Wilson, Nucleic Acids Res. **30**, 3615 (2002).
36. A.M. Kosevich, *The Theory of Crystal Lattice* (Vyshcha Shkola, Kharkov, 1988) (in Russian).
37. N.A. Ismailov, *Electrochemistry of Solutions* (Khimiya, Moscow, 1976) (in Russian).
38. M.V. Volkenshtein, M.A. Eliashevich, and B.I. Stepanov, *Vibrations of Molecules* (Gostekhteorizdat, Moscow-Leningrad, 1949) (in Russian).
39. A.N. Vereshchagin, *Polarizability of Molecules* (Nauka, Moscow, 1980) (in Russian).

Received 07.05.10

#### НИЗЬКОЧАСТОТНІ КОЛИВАННЯ ДНК З МІЖЛАНЦЮЖКОВИМИ ПРОТИІОНАМИ

С.М. Перепелиця, С.Н. Волков

## Резюме

В рамках розвинутої феноменологічної моделі досліджено низькочастотні коливання ДНК з протиіонами, які розташовані між фосфатними групами різних тяжів подвійної спіралі. Розраховано частоти, амплітуди та інтенсивності мод КР ДНК в діапазоні від 10 до 200  $\text{cm}^{-1}$  для випадку протиіонів  $\text{Mg}^{2+}$  у різних положеннях відносно подвійної спіралі (біля фосфатів або між ними). Розрахунки показали, що міжланцюжкові протиіони впливають переважно на моди розтягу водневих зв'язків в парах азотистих основ та моди коливань остова. Використовуючи одержані значення частот та інтенсивностей, побудовано низькочастотні спектри КР Mg-ДНК. Одержані спектри дозволяють визначати положення протиіонів відносно фосфатних груп подвійної спіралі ДНК.